

Internal Biasing in Relaxor Ferroelectric Polymer to Enhance the Electrocaloric Effect

Xiaoshi Qian, Hui-Jian Ye, Tiannan Yang, Wen-Zhu Shao, Liang Zhen, Eugene Furman, Long-Qing Chen, and Qiming Zhang*

The relaxor ferroelectric materials, because of their large and reversible electric field induced polarization, have been demonstrated to possess giant electrocaloric effect (ECE) over a broad temperature range, which are attractive for refrigeration with high energy efficiency and environmental friendliness. However, high electric fields are required to generate the giant ECE in these materials, posing challenge for these materials in practical cooling devices which also require high reliability and low cost. Here, a general approach is reported, for example, establishing an internal bias field in these relaxor ferroelectric polymers, to significantly improve ECE which can be induced at low electric fields. It is demonstrated that in a polymer blend (nanocomposite) with a properly controlled normal ferroelectric in nanophase dispersion in the relaxor polymer matrix, the charge neutrality in the blends can cause an internal biasing field, leading to more than 45% enhancement in the ECE at low electric field ($\approx 50 \text{ MV m}^{-1}$). This internal biasing approach provides a universal strategy to enhance other low field responses such as the electro-mechanical response in relaxor ferroelectrics.

such as electromechanical (EM) sensors and actuators, energy harvesting, and solid-state cooling (through the electrocaloric (EC) effect).^[1–7] In order to generate EM or EC responses, it is highly desirable that a large and reversible polarization change can be induced in the ferroelectric materials. In normal ferroelectric materials, which exhibit square polarization–electric field (P – E) loops, the reversible polarization change is small, as illustrated in Figure 1a.^[1,4,5] On the other hand, by operating near a ferroelectric–paraelectric (FE–PE) phase transition or by utilizing ferroelectric relaxor, a large and reversible polarization change can be induced, see Figure 1a for a relaxor ferroelectric polymer.^[1–4] Indeed, large EM and EC responses have been demonstrated in many materials such as large electrostrictive strain and giant ECE near FE–PE transitions in normal ferroelectric and in relaxor ferroelectrics.^[3–6,8,9]

1. Introduction

Owing to effective couplings of polarization P with many key material parameters such as stress/strain and temperature/entropy, ferroelectric materials are attractive for many applications

From the Landau thermodynamic theory of ferroelectrics, the strain and EC temperature change ΔT are proportional to the square of polarization,^[1,10,11] i.e., $\Delta T \propto P^2$ and hence $\Delta T \propto E^2$ because P is approximately proportional to the applied electric field E provided field is not high enough for nonlinear dielectric susceptibilities to become important contributors to polarizability. In this paper, this class of materials is referred to as the square law materials. The square law dependence on E yields a high EC or EM response at high E fields but when E is low, these responses become small. This is why in many practical device applications, a DC bias field is applied to induce large responses under small AC (or changing fields).^[12] The external DC bias field causes complications in the system design and may also cause dielectric breakdown when the field is too high. On the other hand, if an internal DC bias field E_{bias} can be established in the material, $\Delta T = c(E_{\text{bias}} + E)^2 - cE_{\text{bias}}^2$ is larger than cE^2 when E_{bias} and E have the same polarity (along the same direction), where c is an EC constant, as schematically shown in Figure 1b. The question is whether and how such an E_{bias} be established in the EC materials. We note that in other functional material systems, similar questions have been asked and investigated. For example, in magnetoelectric (ME) composites, utilizing the exchange bias in a multilayer structure, an internal small DC magnetic field (up to 10 mT) was established that eliminated the need of an external DC bias field in the magnetostrictive alloy for the ME composite sensors.^[13]

X. Qian, Prof. Q. M. Zhang
Department of Electrical Engineering
The Pennsylvania State University
University Park, PA 16802, USA
E-mail: qxz1@psu.edu

Dr. H.-J. Ye, Dr. E. Furman
Materials Research Institute
The Pennsylvania State University
University Park, PA 16802, USA

Dr. H.-J. Ye, Prof. W.-Z. Shao, Prof. L. Zhen
School of Materials Science and Engineering
Harbin Institute of Technology
Harbin 150001, China

Dr. H.-J. Ye
College of Materials Science and Engineering
Zhejiang University of Technology
Hangzhou 310014, China

T. Yang, Prof. L.-Q. Chen
Department of Materials Science and Engineering
The Pennsylvania State University
University Park, PA 16802, USA



DOI: 10.1002/adfm.201501840

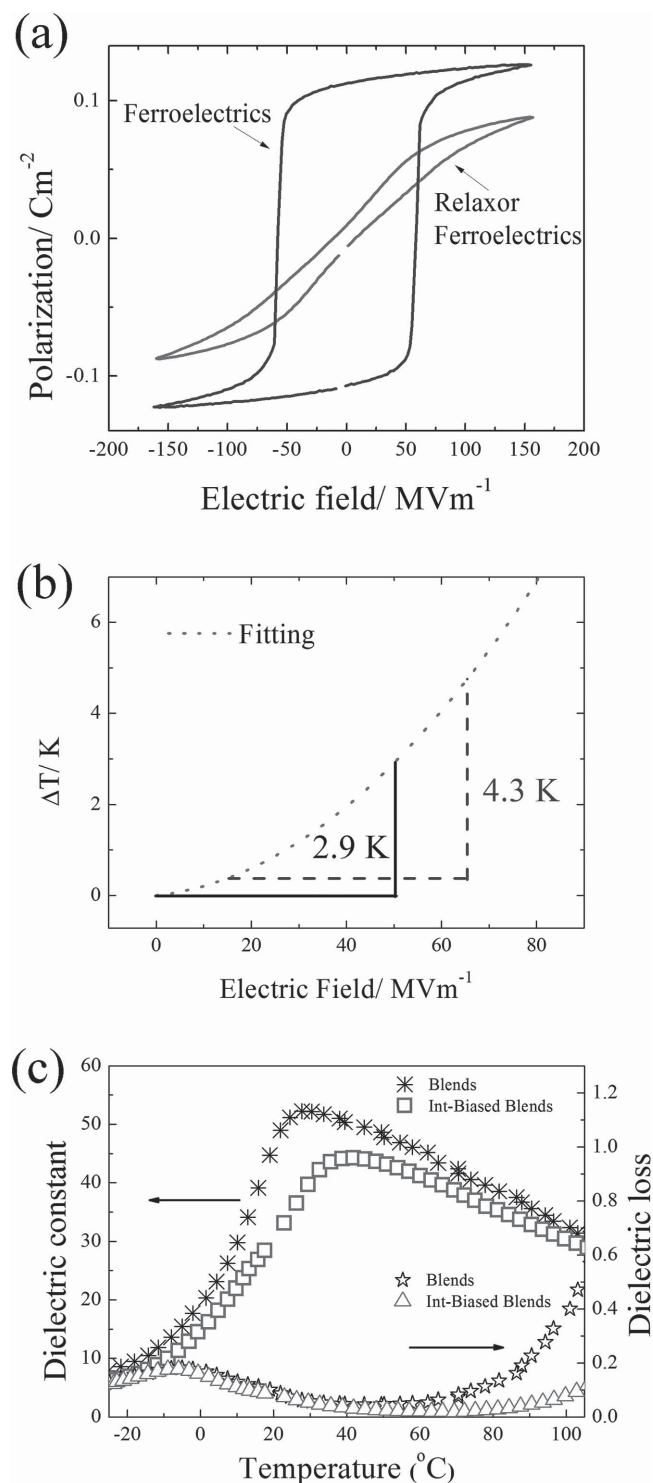


Figure 1. a) The polarization hysteresis (P - E) loops of the normal ferroelectric P(VDF-TrFE) copolymer 65/35 mol% and the relaxor ferroelectric P(VDF-TrFE-CFE) terpolymer. b) Schematic of internal biasing in a square law ECE material. With an internal field of 15 MV m^{-1} , the EC induced ΔT can be enhanced. The nonlinear curve is fitting from field-dependent ECE results in unbiased relaxor ferroelectric polymers. c) The dielectric properties of blend (star) and internal-biased (int-biased) blend (square) as a function of temperature from -30 to 100 $^{\circ}\text{C}$ at 1 kHz .

Analogously, a normal ferroelectric thin film was also utilized in a photovoltaic (PV) device to establish an internal DC bias field in the device and improve the PV cell efficiency.^[14] In this paper, we investigate a polymer blend approach (a nanocomposite approach), in which a normal ferroelectric component in the nanophase form is introduced into the EC relaxor polymer, and demonstrate that an internal DC bias field can be established in the blends by properly controlling the properties of the normal ferroelectric component. As a result, the EC response at low electric fields is enhanced markedly, i.e., a $\Delta S = 24.5 \text{ J kg}^{-1} \text{ K}^{-1}$ and $\Delta T = 4.9 \text{ K}$ can be induced under 50 MV m^{-1} at 40 $^{\circ}\text{C}$, which is more than 45% higher than that in the blends without internal bias field ($\Delta S = 16.7 \text{ J kg}^{-1} \text{ K}^{-1}$ and $\Delta T = 3.3 \text{ K}$).

2. Results and Discussion

The P(VDF-TrFE-CFE) (poly(vinylidene fluoride-trifluoroethylene-chlorofluoroethylene)) 59/33/8 mol% relaxor terpolymer was chosen for the study, because of its high EC response.^[15] Figure 1a is the polarization loop of this terpolymer at room temperature, showing large and reversible polarization changes. Normal ferroelectric P(VDF-TrFE) was employed in the blends to induce internal DC bias. The copolymers in compositions from 50/50 to 100/0 mol% (PVDF homopolymer) with weight percent from 5 to 30 wt% in the blends were studied in order to examine how the copolymer composition (and hence the strength of normal ferroelectricity) and volume content influence the EC response and internal DC bias fields. The normal ferroelectric P(VDF-TrFE) does not show a high EC response except near the FE-PE transition and excess amount of P(VDF-TrFE) in the blends hence will reduce the EC response in the temperature of study, i.e., near room temperature.

Experimental results reveal that both the composition and concentration of the normal ferroelectric component affect the establishment of the internal bias field and EC response of the blend, indicating the delicate balance between the normal ferroelectric component which shows very weak EC response and relaxor ferroelectric which requires high fields to establish large EC response. Experimental results also show that terpolymer/copolymer blends display higher polarization (and EC) response compared with the neat terpolymer when the copolymer VDF/TrFE ratio is below 85/15 mol%. The blends with copolymers at VDF/TrFE ratio higher than 85/15 mol% exhibit lower polarization (and EC) response (Figure S1, Supporting Information). Among all the blends investigated, the one with 65/35 mol% P(VDF-TrFE) at 10 wt% concentration exhibits the highest EC response. Hence, blends of this composition (blends with 90/10 wt% of terpolymer/copolymer) are investigated further on how to establish an E_{bias} so that a high EC response can be obtained at low electric fields. The results presented in the paper are for this terpolymer/copolymer blend except if otherwise specified. The normal ferroelectric P(VDF-TrFE) 65/35 mol% copolymer exhibits a near square polarization loop at room temperature, as shown in Figure 1a.

The dielectric properties of the blend are shown in Figure 1c, which exhibit a broad dielectric constant peak and typical relaxor dispersion. Indeed, the FT-IR spectra of the

blends do not display absorptions from the all-trans bonds of the normal ferroelectric phase (see Figure S2, Supporting Information). This is consistent with earlier experimental results, indicating that ferroelectric copolymer P(VDF-TrFE) in the blends at low wt% (e.g., 10 wt%) forms nanophase dispersion in the relaxor terpolymer matrix and does not show normal ferroelectric characteristics.^[16] To induce an E_{bias} in the terpolymer, the preferentially oriented polarization of the normal ferroelectric P(VDF-TrFE) component in the blends should be established so that an internal field can be induced in the terpolymer, even in the absence of external electric field. In our study, it was found that poling the blends by applying a DC field of 50 MV m^{-1} at 85°C , which is above the FE-PE transition of the 65/35 mol% copolymer, for more than 10 min on the blend film and then cooling down the film under the field at 1°C min^{-1} to room temperature yielded significantly enhanced EC responses at low fields.^[17] Increasing the DC poling field beyond 50 MV m^{-1} and/or to higher temperature did not make much difference in the EC response for blends at this composition of blends. In this paper, the blends with an E_{bias} are referred to as the internal-biased (int-biased) blends, in contrast to the blends which are not poled. The results presented in this paper on the int-biased blends were obtained after the external DC fields were removed at room temperature for more than 1 d.

Both the dielectric and polarization responses indicate the presence of a DC bias field for the int-biased blends. For instance, the int-biased blend films exhibit a broad dielectric peak which is at higher temperature compared with the unbiased blend films. Earlier experiments have shown that applying DC fields to relaxor ferroelectric moves the broad dielectric peak to higher temperature while also reducing the dielectric peak height, consistent with observed results for the int-biased blends.^[4,18] In addition, the dielectric loss at high temperatures is also reduced markedly, for example, from 40% loss of the unbiased blends to below 10% for the int-biased blends at 100°C . The increased dielectric loss at high temperature originates mainly from the increase in the conduction loss. The experimental data indicate that the int-biased blends can effectively cut down the conduction loss in the films, which is likely due to the presence of internal polar interfaces in the blends between the copolymer and terpolymer in the int-biased blends, that block the space charge conduction.^[19] An $E_{\text{bias}} \approx 14 \text{ MV m}^{-1}$ can be seen in the bipolar P - E loop in Figure 2a as the center of the loop is shifted horizontally. The establishment of an effective DC bias field in the blends was confirmed by the FT-IR spectra, Figure S2 (Supporting Information), where an absorption peak corresponding to the all-trans polar conformation (at 1280 cm^{-1}) is observed for the int-biased blend films.

To further study the internal bias field and its influence on the polarization and EC response, unipolar P - E loops were measured along the same direction as the E_{bias} direction to investigate the polarization change in a heating-cooling cycle (measured at 10 Hz) and presented in Figure 2b. Figure 2c summarizes the increased polarization in the unipolar P - E loops under different applied fields in the int-biased blends, compared with that of unbiased blends. The int-biased blends display higher polarization level, especially at low field range.

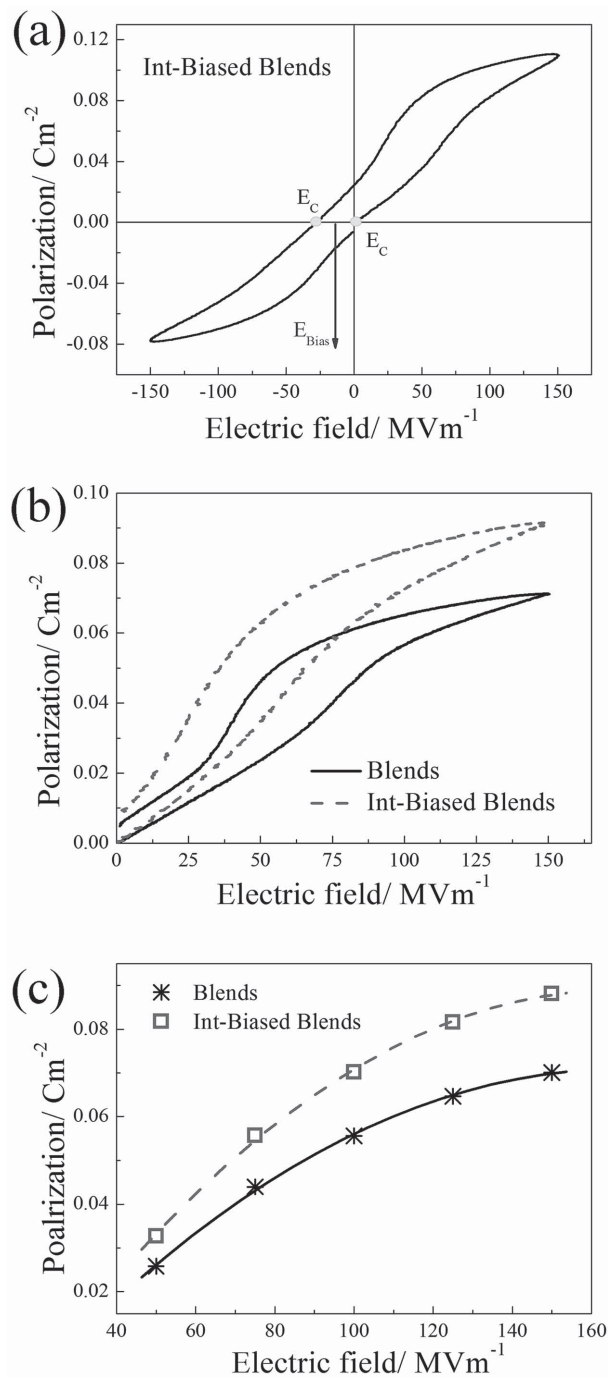


Figure 2. The P - E loops of blend with the internal bias field. a) The bipolar P - E loop of int-biased samples measured at room temperature. The data reveal a shift of electric field due to the internal DC biasing in the blend. b) Comparison of the unipolar P - E loops of int-biased blend with that of the blend under 100 MV m^{-1} . c) Comparison of the maximum polarizations of blend (star) and int-biased blend (square) from the unipolar P - E loops as functions of electric fields measured at 25°C . The curves are drawn to guide eyes. The P - E loops were measured at 10 Hz.

The EC responses (the adiabatic temperature change ΔT and isothermal entropy change ΔS) of both int-biased and unbiased blends under electric fields of $\Delta E = 50$ and 100 MV

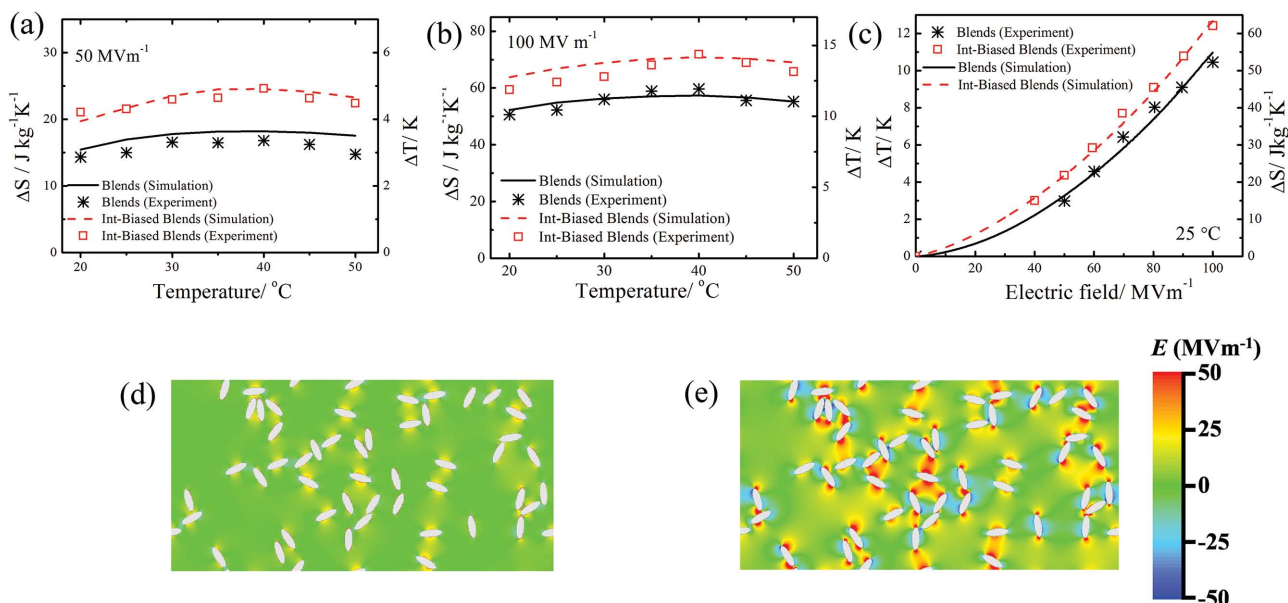


Figure 3. The improvement of the ECE performance in the blends due to the internal biasing: the adiabatic temperature change ΔT , isothermal entropy change ΔS of int-biased blend (squares) and blend (stars). a,b) EC induced ΔS and ΔT as functions of temperature under electric fields of 50 and 100 MV m⁻¹, respectively. c) ΔT and ΔS as functions of electric field measured at room temperature. The solid and dashed lines depict phase field simulation results. Internal field distribution inside the relaxor/ferroelectric polymer blend d) before int-biasing and e) after int-biased under 50 MV m⁻¹.

m⁻¹, respectively, as functions of temperature are presented in Figure 3a,b.^[15] A marked enhancement (more than 45%) of the EC responses is obtained at 50 MV m⁻¹ where the peak values of $\Delta T = 4.9$ K and $\Delta S = 24.5$ J kg⁻¹ K⁻¹ are obtained for the int-biased blends, compared with the peak values of $\Delta T = 3.3$ K and $\Delta S = 16.7$ J kg⁻¹ K⁻¹, for unbiased blends at 40 °C. Presented in Figure 3c are the EC responses as functions of the applied field at room temperature (25 °C). As can be seen, the EC response of the int-biased blends under 50 MV m⁻¹ is the same as that of unbiased blends under 62 MV m⁻¹, which is consistent with that observed from the bipolar P - E loop in Figure 2a. The enhancement, which is more prominent at lower field, opens up opportunities to design EC based cooling devices with capabilities in low-field and reliable operation.

For clearer illustration, we performed phase-field modeling to the unbiased and int-biased blends, and simulated the EC responses. Phase-field method provides powerful computational approach to modeling the ferroelectric domain evolution at given external fields,^[20] which can predict both the microstructure and the properties of a composite system. Figure 3d,e shows the distribution of remnant electric field established under an external $\Delta E = 100$ MV m⁻¹ in the terpolymer matrix which is unbiased and int-biased with $E_{\text{bias}} = 50$ MV m⁻¹, respectively. As seen, while the unbiased blends at remnant show very weak internal electric field, the int-biased blends exhibit a marked internal electric field in the terpolymer matrix, which is especially concentrated in regions around the copolymer phase regions, due to the presence of a strong remnant polarization in the ferroelectric copolymer. As a result, the int-biased blends exhibit an effective internal electric field bias of around 14 MV m⁻¹ compared to the unbiased blends. The ECE of the blends is further enhanced by the electric field bias (see the solid and dashed lines in Figure 3a-c), which is consistent with the experiment observation.

In order to understand the influence of internal E_{bias} on the polarization and EC responses, the β coefficient, from $\Delta S = -\frac{1}{2}\beta P^2$, is evaluated for the blends, using the data in Figures 2 and 3, and presented in Figure 4a. The internal DC bias field enhances β at low electric fields (<40 MV m⁻¹), while at high fields, β of the int-biased blends becomes smaller than that of unbiased blends. The results indicate that the internal E_{bias} approach indeed enhances ECE more effectively at low electric fields ($\Delta E < 50$ MV m⁻¹).

Besides the peak ECE that an EC material can generate, high electrocaloric coefficients, such as $\Delta T/\Delta E$ and $\Delta S/\Delta E$, are also critical in order to measure EC behaviors versus different external electric fields. $\Delta S/\Delta E$ and $\Delta T/\Delta E$ for the int-biased blends and unbiased blends at different applied field are presented in Figure 4b, which shows a large improvement compared with that of the unbiased blends, especially at low electric fields. These parameters are summarized in Table 1 and compared with other state-of-the-art stand-alone EC materials reported in the literature (including the measuring fields and temperatures).^[21–25] The $\Delta S/\Delta E$, which is measured in int-biased polymer blend, is comparable to those reported in inorganic ceramics and single crystals. The improvement of more than 45% in both ECE ($\Delta T = 4.9$ K) and EC coefficient ($\Delta S/\Delta E = 0.49 \times 10^{-6}$ J m kg⁻¹ K⁻¹ V⁻¹) at 50 MV m⁻¹, which is far away from the breakdown field of such polymer blends, suggests that a more effective, efficient, and reliable electric operation on such material is achievable.

3. Conclusion

The results indicate that with better understanding of how polarizations contribute to ECE induced entropy change, much

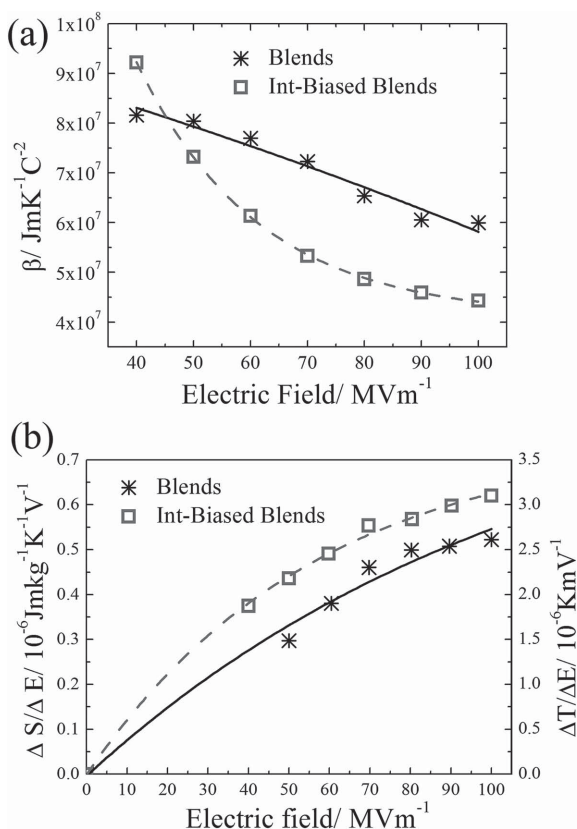


Figure 4. The EC performances of the int-biased blends and blends at room temperature. a) Coefficient β as functions of electric field and b) the EC coefficient $\Delta S/\Delta E$ and $\Delta T/\Delta E$. Data points are shown and the curves are drawn to guide eyes.

larger ECE at lower electric fields could be achieved. Moreover, the work presented here represents a general approach to improve the performance of square law materials at low applied fields. This work as well as a plethora of progresses made recently in EC materials suggest there are opportunities for further improving ECE as we develop our understanding of ECE and polar dielectrics.

4. Experimental Section

P(VDF-TrFE-CFE) terpolymer (59/33/8 mol%) was synthesized with suspension polymerization process by Piezotech (France) and P(VDF-TrFE) (65/35 mol%) was supplied by Solvay (Belgium). The density of the copolymer and terpolymer is nearly the same ($\approx 1.75 \text{ g cm}^{-3}$). The films were fabricated via solution casting method. The P(VDF-TrFE-CFE) and P(VDF-TrFE) were initially dissolved in *N,N*-dimethylformamide (DMF) solvent, respectively. Then the solutions with proper weight ratio were mixed and stirred for overnight at room temperature. The final solution was filtered with $0.2 \mu\text{m}$ sized polytetrafluoroethylene (PTFE) filters before pouring on glass plate, which was dried at 70°C for 12 h and cooled slowly to room temperature. The films after peeling off from the plates were annealed at 100°C for 12 h to further remove the residual solvent and increase the crystallinity. The thickness of the blend films is around $6.0 \mu\text{m}$. Sputtered gold films of 20 nm thick were used as the electrodes. The dielectric property versus temperature was characterized by an LCR meter (HP4284A) equipped with a computer controlled temperature chamber (Delta 9023). *P-E* loops were measured using a Sawyer-Tower circuit. The ECE of samples was directly measured by a specially designed setup in which the heat Q absorbed or ejected from the film due to ECE was measured by a heat flux sensor, as well as by direct comparison with a reference heat (calorimetry method), with a voltage supply system for various applied voltage waveforms and a temperature controlled chamber where temperature can be controlled better than 0.1°C , which has been described in detail in refs. [15,20], and [21]. The directly measured heat flux signals for unbiased and

Table 1. Comparison of the electrocaloric properties among different materials.

| Material ^{a)} | Form | $T [^\circ\text{C}]$ | ΔE [MV m^{-1}] | ΔS [$\text{J kg}^{-1} \text{K}^{-1}$] | $\Delta S/\Delta E$ [$10^{-6} \text{ J m kg}^{-1} \text{K}^{-1} \text{V}^{-1}$] | Ref. |
|------------------------|--------------------------|----------------------|--------------------------------------|--|--|-----------|
| Int-biased blends | Polymer | 40 | 50 | 24.5 | 0.49 | This work |
| Blends | Polymer | 38 | 50 | 16.7 | 0.33 | This work |
| Int-biased blends | Polymer | 40 | 100 | 72 | 0.72 | This work |
| Blends | Polymer | 38 | 100 | 60 | 0.60 | This work |
| P(VDF-TrFE-CFE) | Polymer | 30 | 50 | 8.9 | 0.18 | [15] |
| P(VDF-TrFE-CFE) | Polymer | 30 | 100 | 37.8 | 0.38 | [15] |
| P(VDF-TrFE-CFE) | Polymer | 30 | 150 | 73.5 | 0.49 | [15] |
| Irradiated P(VDF-TrFE) | Polymer | 50 | 100 | 50 | 0.50 | [21] |
| Irradiated P(VDF-TrFE) | Polymer | 50 | 180 | 160 | 0.89 | [21] |
| BZT ($x = 0.2$) | Ceramic | 39 | 14.5 | 8 | 0.54 | [22] |
| BZT ($x = 0.2$) | Ceramic | 38 | 2.1 | 1.95 | 0.93 | [22] |
| BZT ($x = 0.15$) | Ceramic | 69 | 15 | 7.3 | 0.5 | [22] |
| BT | Cera. MLCC ^{b)} | 80 | 80 | 10.1 | 0.13 | [23] |
| PMN | Ceramic | 67 | 9 | 2.5 | 0.28 | [24] |
| PMN-30PT | Ceramic | 145 | 9 | 2.1 | 0.23 | [24] |
| BT | Sing. cryst. | 129 | 1.2 | 2 | 0.79 | [25] |

^{a)} T is the temperature where the ECE was measured, ΔE is the applied field, and $\Delta S/\Delta E$ is field dependent; ^{b)} MLCC refers to the multilayer ceramic capacitor.

int-biased blend are shown in Figure S3 (Supporting Information) under $\Delta E = 50$ and 100 MV m^{-1} , respectively.

Phase-Field Modeling: The total size of the simulation system is $4 \times 2 \mu\text{m}^2$, which was discretized into a 2D array of 800×400 cells. A nonevolving two-phase composite structure with a sharp interface was considered, where blends composed of a P(VDF-TrFE-CFE) matrix was filled with randomly oriented and randomly distributed elliptical P(VDF-TrFE) particles with the size of $80 \times 240 \text{ nm}^2$. The size and distribution of particles were determined by atomic force microscopy in comparing same area under height and modulus mode (Figure S4, Supporting Information). P(VDF-TrFE) copolymer, which exhibits higher modulus (brighter parts shown in modulus mode), can be seen randomly oriented and distributed in polymer matrix with the size around $50\text{--}100 \times 150\text{--}250 \text{ nm}$. The orientation and distribution (position of the copolymer) were decided by random numbers that were generated by FORTRAN code. The evolution of electric polarization field $\mathbf{P}(\mathbf{r}, t)$ in the composite responsive to an applied external electric field \mathbf{E}_{ext} was modeled through solving the time-dependent Ginzburg–Landau equation^[20,26] $\partial \mathbf{P} / \partial t = -L \cdot (\delta F / \delta \mathbf{P})$ using a semi-implicit Fourier-spectral method.^[27] L is the kinetic coefficient related to ferroelectric domain evolution. F is the Gibbs free energy of the composite, expressed as^[26]

$$F(\mathbf{P}, \mathbf{E}_{\text{ext}}, T) = \int \left[f_{\text{Land}}(\mathbf{P}, T) + f_{\text{grad}}(\mathbf{P}) + \frac{1}{2} \epsilon_0 \mathbf{E}_{\text{d}}^2 - \mathbf{P} \cdot \mathbf{E}_{\text{ext}} \right] d\mathbf{r}^3 \quad (1)$$

where f_{Land} is the Landau free energy density; $f_{\text{grad}}(\mathbf{P}) = \mathbf{g}(\nabla \mathbf{P})^2$ is the gradient energy density, \mathbf{g} being the gradient energy coefficient; \mathbf{E}_{d} and ϵ_0 are the depolarization field and the vacuum permittivity, respectively. The Landau potential is expanded to a sixth-order polynomial as $f_{\text{Land}}^{\text{C}}(\mathbf{P}, T) = a_{\text{f}}^{\text{C}} \mathbf{P}^2 + a_{\text{f}}^{\text{C}} \mathbf{P}^4 + a_{\text{f}}^{\text{C}} \mathbf{P}^6$ for the ferroelectric copolymer and to a second-order polynomial^[28] $f_{\text{Land}}^{\text{T}}(\mathbf{P}, T) = \mathbf{P}^2 / (2\epsilon_0 \kappa_{\text{r}}^{\text{T}})$ for the relaxor terpolymer, respectively; a and κ_{r} are Landau energy coefficients and the relative dielectric permittivity, respectively. \mathbf{E}_{d} is obtained by solving the electrostatic Poisson equation $\nabla \cdot (\epsilon_0 \mathbf{E} + \mathbf{P}) = 0$ using a Fourier-spectral method.^[29] Through tracking the change of thermodynamic Gibbs free energy during microstructural evolution, the effective ECE of the composite is evaluated following the thermodynamic relation $S = -k(\partial F / \partial T)_{\text{E}}$, where k is a scaling factor. The internal biasing is considered as a residual electric field in the ferroelectric copolymer phase with the magnitude of 30% of the field established during internal biasing. The material constants and simulation parameters are listed as ref. [30].

Supporting Information

Supporting Information is available from the Wiley Online Library or from the author.

Acknowledgements

X.Q. and H.-J.Y. contributed equally to this work. The authors thank Rasa Pirc for valuable discussions. The works by X.Q. and H.-J.Y. were supported by the U.S. DoE, Office of Basic Energy Sciences, Division of Materials Science and Engineering under Award No. DE-FG02-07ER46410. T.Y. and L.-Q.C. were supported by the U.S. NSF under Grant No. DMR-1410714.

Received: May 4, 2015

Revised: June 15, 2015

Published online: July 14, 2015

- [1] M. Lines, A. Glass, *Principles and Applications of Ferroelectrics and Related Materials*, Clarendon, Oxford 1977.
- [2] J. F. Scott, *Science* **2007**, 315, 954.
- [3] K. Uchino, *Am. Ceram. Soc. Bull.* **1986**, 65, 647.
- [4] L. E. Cross, *Ferroelectrics* **1987**, 76, 241.
- [5] Q. M. Zhang, V. Bharti, X. Zhao, *Science* **1998**, 280, 2101.
- [6] B. Neese, B. Chu, S.-G. Lu, Y. Wang, E. Furman, Q. M. Zhang, *Science* **2008**, 321, 821.
- [7] Y. M. Liu, K. L. Ren, H. F. Hofmann, Q. M. Zhang, *IEEE Trans. Ultrason. Ferroelectr. Freq. Control* **2005**, 52, 2411.
- [8] A. S. Mischenko, Q. Zhang, J. F. Scott, R. W. Whatmore, N. D. Mathur, *Science* **2006**, 311, 1270.
- [9] S. G. Lu, B. Rozic, Q. M. Zhang, Z. Kutnjak, B. Neese, *Appl. Phys. Lett.* **2011**, 98, 122906.
- [10] R. Pirc, Z. Kutnjak, R. Blinc, Q. M. Zhang, *J. Appl. Phys.* **2011**, 110, 074113.
- [11] S.-G. Lu, Q. Zhang, *Adv. Mater.* **2009**, 21, 1983.
- [12] K. Uchino, *Ferroelectric Devices*, Marcel Dekker, New York 2000.
- [13] E. Lage, C. Kirchhof, V. Hrkac, L. Kienle, R. Jahns, R. Knochel, E. Quandt, D. Meyners, *Nat. Mater.* **2012**, 11, 523.
- [14] Y. B. Yuan, T. J. Reece, P. Sharma, S. Poddar, S. Ducharme, A. Gruverman, Y. Yang, J. S. Huang, *Nat. Mater.* **2011**, 10, 296.
- [15] X. Li, X.-S. Qian, S. G. Lu, J. Cheng, Z. Fang, Q. M. Zhang, *Appl. Phys. Lett.* **2011**, 99, 052907.
- [16] X.-Z. Chen, X. Li, X.-S. Qian, S. Wu, S.-G. Lu, H.-M. Gu, M. Lin, Q.-D. Shen, Q. M. Zhang, *Polymer* **2013**, 54, 2373.
- [17] A. J. Lovinger, T. Furukawa, G. T. Davis, M. G. Broadhurst, *Ferroelectrics* **1983**, 50, 553.
- [18] Y. Zhang, J. M. Tian, L. T. Li, Z. L. Gui, *J. Mater. Sci.: Mater. Electron.* **2000**, 11, 347.
- [19] K. C. Kao, *Dielectric Phenomena in Solids*, Academic Press, 2004.
- [20] L.-Q. Chen, *J. Am. Ceram. Soc.* **2008**, 91, 1835.
- [21] X. Li, X.-S. Qian, H. Gu, X. Chen, S. G. Lu, M. Lin, F. Bateman, Q. M. Zhang, *Appl. Phys. Lett.* **2012**, 101, 132903.
- [22] X.-S. Qian, H.-J. Ye, Y.-T. Zhang, H. Gu, X. Li, C. A. Randall, Q. M. Zhang, *Adv. Funct. Mater.* **2014**, 24, 1300.
- [23] Y. Bai, G. P. Zheng, K. Ding, L. J. Qiao, S. Q. Shi, D. Guo, *J. Appl. Phys.* **2011**, 110, 094103.
- [24] B. Rozic, M. Kosec, H. Ursic, J. Holc, B. Malic, Q. M. Zhang, R. Blinc, R. Pirc, Z. Kutnjak, *J. Appl. Phys.* **2011**, 110, 064118.
- [25] X. Moya, E. Stern-Taulats, S. Crossley, D. Gonzalez-Alonso, S. Kar-Narayan, A. Planes, L. Manosa, N. D. Mathur, *Adv. Mater.* **2013**, 25, 1360.
- [26] Y. L. Li, S. Y. Hu, Z. K. Liu, L. Q. Chen, *Acta Mater.* **2002**, 50, 395.
- [27] L. Q. Chen, J. Shen, *Comput. Phys. Commun.* **1998**, 108, 147.
- [28] T. N. Yang, J.-M. Hu, C. W. Nan, L. Q. Chen, *Appl. Phys. Lett.* **2014**, 104, 052904.
- [29] Y. L. Li, S. Y. Hu, Z. K. Liu, L. Q. Chen, *Appl. Phys. Lett.* **2002**, 81, 427.
- [30] For P(VDF-TrFE):
 $a_{\text{f}}^{\text{C}} = 1.412 \times 10^7 (T/^{\circ}\text{C} - 42) \text{ C}^{-2} \text{ m}^2 \text{ N}$, $a_{\text{f}}^{\text{T}} = 1.842 \times 10^{11} \text{ C}^{-4} \text{ m}^6 \text{ N}$,
 $a_{\text{f}}^{\text{C}} = 2.585 \times 10^{13} \text{ C}^{-6} \text{ m}^{10} \text{ N}$, $g_{11}^{\text{C}} = 5 \times 10^{-7} \text{ C}^{-2} \text{ m}^4 \text{ N}$,
 $g_{44}^{\text{C}} = g_{44}^{\text{m}} = 2.5 \times 10^{-7} \text{ C}^{-2} \text{ m}^4 \text{ N}$;
For P(VDF-TrFE-CFE):
 $\kappa_{\text{r}}^{\text{T}} = 68.8 - 0.412 T/^{\circ}\text{C} - 6.20 \times 10^{-3} (T/^{\circ}\text{C})^2$
 $+ 5.26 \times 10^{-5} (T/^{\circ}\text{C})^3 (15^{\circ}\text{C} \leq T \leq 70^{\circ}\text{C})$, $g^{\text{T}} = 0$; $k = 2.56$.